

**Adenosine Monophosphate Activated Protein Kinase Induces Cholesterol Efflux
from Macrophage-Derived Foam Cells and Alleviates Atherosclerosis in
Apolipoprotein E-Deficient Mice**

Running title: AMPK and cholesterol efflux from foam cells

Dan Li^{1,2,3}, Duan Wang^{2,3}, Yun Wang^{2,3}, Wenhua Ling^{1,2}, Xiang Feng^{1,2}, Min Xia^{1,2,*}

¹ Guangdong Provincial Key Laboratory of Food, Nutrition and Health

² Department of Nutrition, School of Public Health, Sun Yat-sen University (Northern Campus), Guangzhou, Guangdong Province, P.R.China, 510080

³ These authors contributed equally to these work.

* Address correspondence to: Mia Xia, Ph.D., Department of Nutrition, School of Public Health, Sun Yat-sen University (Northern Campus), 74 Zhongshan Road 2, Guangzhou, Guangdong Province, P.R.China, 510080. Phone: 86-20-87332433, Fax: 86-20-87330446; E-mail: xiamin@mail.sysu.edu.cn

Increasing evidence suggests that adenosine monophosphate activated protein kinase (AMPK) exerts protective effects for cardiovascular diseases apart from the regulation of energy homeostasis. However, the role of AMPK and its underlying mechanism on macrophage foam cell formation are poorly understood. In this study, we sought to investigate the potential effects of AMPK in modulating cholesterol deposition by using murine macrophage-derived foam cells. Incubation with 5-aminoimidazole-4-carboxamide ribonucleoside (AICAR) markedly attenuated the cholesterol ester accumulation in oxidized low density lipoprotein (OxLDL)-loaded macrophages. Notably, AICAR treatment significantly increased ATP-binding cassette transporters G1 (ABCG1) mRNA and protein levels without affecting mRNA and protein expression of ABCA1, scavenger receptors, including scavenger receptor-A (SR-A), CD36, and scavenger receptor-BI (SR-BI), and cholesterol synthesis-related genes. The upregulation of ABCG1 by AICAR was independent on liver X receptor/ retinoid

X receptor (LXR/RXR) pathway but dependent on external signal regulated kinase (ERK) activation. AICAR elevates ABCG1 expression through a post-transcriptional mechanism that stabilizes the mRNA. Using a heterologous system with luciferase as a reporter, we further identify the ABCG1 mRNA 3' untranslated region (3'-UTR) responsible for the regulatory effect of AICAR. Prevention of ABCG1 expression by small interfering RNA abolished the AICAR-mediated attenuation on foam cell formation. Furthermore, increased ABCG1 expression and reduced lipid accumulation were demonstrated in AICAR treated-macrophages isolated from apolipoprotein E-deficient mice (apoE^{-/-} mice). AICAR treatment also inhibited atherosclerotic plaque formation in apoE^{-/-} mice. Our findings elucidate a precise mechanism involved in the prevention of atherogenesis by AMPK.

INTRODUCTION

Atherosclerosis is a leading cause of illness and death worldwide. The differentiation of macrophages into lipid-laden foam cells is a crucial process during the development of atherosclerosis (1-3). The transformation of foam cells is due mainly to dysregulated uptake of modified low-density lipoprotein (LDL) by macrophages, resulting in excessive deposition of lipoprotein-derived cholesterol inside the cells (4,5). Traditionally, it has been assumed that the uncontrolled uptake of oxidized low density lipoproteins (OxLDL) by macrophage scavenger receptors is largely responsible for this process. Several members of macrophage scavenger receptors including class A SRs (SR-AI) and class B SRs (such as SR-BI and CD36) has been implicated in the formation of foam cells by its capacity to bind and endocytose OxLDL, and shown to play a critical role in the development of atherosclerotic lesions (6,7). On the contrary, cholesterol efflux is regarded as the most important keypoint with regard to maintenance of cholesterol homeostasis and

atherosclerosis.

Two major potential cholesterol efflux pathways from macrophages have been described: SR-BI-mediated cholesterol efflux, and active cholesterol efflux mediated by the ATP-binding cassette transporters ABCA1 and ABCG1. ABCA1 promotes efflux of phospholipids and cholesterol to lipid-poor apoA-I in a process that involves the direct binding of apoA-I to the transporter. SR-BI and ABCG1 were identified as the key mediators of macrophage cholesterol efflux to mature HDL (8-10). The intracellular cholesterol homeostasis in macrophages is dynamically regulated by cholesterol uptake and cholesterol efflux, processes that are tightly controlled by these receptors.

Adenosine monophosphate activated protein kinase (AMPK), which is expressed in most mammalian cell types, including the vascular cells such as endothelial cells, smooth muscle cells and macrophages, plays a central role in the regulation of energy metabolism under stress conditions (11,12). Activation of AMPK leads to the phosphorylation of a number of key

enzymes in metabolic pathways, such as acetyl-coenzyme A (acetyl-CoA) carboxylase (ACC) or mTOR (mammalian target of rapamycin), by modulating their activities, and by regulating the activity of transcription factors and transcriptional cofactors (13,14). Additionally, AMPK has been reported to exert multiple protective effects in vascular cells by inhibiting inflammation, oxidant production, vascular smooth muscle cell proliferation, and insulin resistance (15,16). However, little is known about the influence of AMPK on foam cell formation. The purpose of this study was to investigate the impact of AMPK on macrophage foam cell formation and its molecular mechanisms.

EXPERIMENTAL PROCEDURES

Materials—AMPK agonist 5-aminoimidazole-4-carboxamide ribonucleoside (AICAR), anti-phospho-AMPK Thr-172 and anti- β -actin were purchased from Cell Signaling Technology. AMPK inhibitor-compound C and LXR α antagonist-geranylgeranyl pyrophosphate ammonium salt (GGPP)

were obtained from Calbiochem (San Diego, Calif). A-769662, a cell permeable drug that potently activates AMPK in cells, was provided by Symansis Pty Ltd (Washdyke, New Zealand). Human 3,3'-dioctadecylindocarbocyanine labeled-fluorescent high density lipoprotein (DiI-HDL) was obtained from Biomedical Technologies Inc. RPMI 1640 culture medium and fetal bovine serum (FBS) was provided by GIBCO. (Grand Island, NY). GW3965, metformin, $1\alpha,25\text{-}[\text{}^3\text{H}]\text{cholesterol}$, actinomycin D, HDL and penicillin/streptomycin were purchased from Sigma-Aldrich (St. Louis, MO).

Cell Culture—Murine macrophage J774.A1 cells (ATCC, TIB-67) were cultured in RPMI 1640 medium supplemented with 10% FBS, penicillin, and streptomycin.

LDL Modification—LDL was isolated from fresh plasma of healthy subjects as previously described (17). LDL was exposed to 5 μM CuSO_4 for 24 h at 37°C; then, Cu^{2+} was removed by extensive dialysis with phosphate-buffered saline (PBS) overnight. The extent of modification

was determined by measurement of thiobarbituric acid–reactive substances. The protein concentration was determined by a Lowry assay (17). OxLDL containing 20 to 50 nM thiobarbituric acid–reactive substances defined as malondialdehyde equivalents per milligrams of LDL protein was used for further experiments (18).

Oil Red O Staining—The macrophages were fixed with 4% paraformaldehyde and then stained by 0.5% Oil Red O. Hematoxylin was used as a counterstain. The density of lipid content was measured with a microplate reader (absorbance at 540 nm, BioTek Instruments Inc) after alcohol extraction (18).

Filipin staining—Macrophages were pretreated with AICAR (1 mM) for 24 h. Then, the cells were loaded with OxLDL (50 µg/ml) in RPMI 1640 medium supplemented with 1% Nutridoma for 24 h. After incubation, cells were rinsed twice with ice-cold PBS and fixed with paraformaldehyde (4% in PBS) for 30 min at 4°C before being incubated with filipin (50 µg/ml in PBS) for 30 min at room temperature. Labelling was then visualised by a fluorescent microscope

(NIKON ECLIPSE TI-E) and fluorescent signals were quantified (19).

Intracellular Lipid Analysis in Macrophages—Intracellular lipids in macrophages were extracted with hexane/isopropanol (3:2) after 24 h incubation with the vehicle or AICAR, evaporated and dissolved in isopropanol containing 10% Triton X-100 for preparation of a sample solution. Free cholesterol and total cholesterol were determined by commercial assay systems (Wako chemicals). Cholesterol ester was estimated by subtracting free cholesterol from total cholesterol. Data are normalized to cellular protein content (20).

Cholesterol Efflux Assays—Adherent macrophages were incubated in RPMI 1640 with OxLDL (50 µg/ml) at 37°C for 24 h to induce macrophage foam cells. The cells were then washed in ice-cold PBS and incubated with AICAR in medium containing 0.2% low endotoxin fatty-acid-free bovine serum albumin (BSA) for the indicated time. After then, cells were washed three times in PBS, and HDL-mediated cholesterol efflux studies were immediately performed by adding fresh

medium in the presence or absence of HDL (10 µg/ml) for 24 h. At the end of this incubation, lipids of cells and media were separately extracted in chloroform and methanol, and then the samples were dried under nitrogen, and free cholesterol and total cholesterol were measured by enzymatic assays. Cholesterol ester was determined as the difference between total and free cholesterol. Cellular proteins were collected by digestion in NaOH and measured by using the Bradford method. The percent change of intracellular cholesterol amounts in the presence of HDL relative to HDL-free culture medium was determined as the percent counts in medium over counts in medium + cells. Each assay was performed in triplicate (20).

In the experiments with [³H]cholesterol, macrophages were incubated for 24 h in RPMI 1640 supplemented with 5% LPDS, 1.0 µCi/ml of [³H]-cholesterol and 50 mg/ml of OxLDL in the absence or presence of AICAR (0.5~2 mM) for 24 h. To equilibrate cholesterol pools, cells were washed twice with PBS and incubated for 24 h in RPMI 1640 containing 0.2%

BSA with no lipoproteins. Cells were washed again and incubated in RPMI 1640 containing 0.2% BSA in the absence or presence of HDL (50 µg/ml) for 24 h. The percentage cholesterol efflux was calculated by dividing the media-derived radioactivity by the sum of the radioactivity in the media and the cells (21).

Cytotoxicity Tests—Cells were grown in microtiter plates and subjected to the experimental culture conditions and treatments as described for efflux experiments. 0.5 mg/ml MTT was added to each well and incubated for 4 h in the cell culture incubator. Solubilization buffer (10% SDS in 0.01 M HCl) was added to each well and incubated in cell culture incubator overnight. Absorbance was measured at 550 nm on a microtiter plate reader. Percent MTT cleavage was determined as follows: (treatment value-media with vehicle value)/(0.1% Triton X-100 value-media with vehicle value) ×100 (22). A lactate dehydrogenase release assay was performed according to the manufacturer's instructions (Biovision, PA).

Quantitative

Real-Time

RT-PCR—Total RNA was extracted from the cultured cells using TRIzol reagent according to the protocol provided by the manufacturer (Life Technologies). Real-time quantitative PCR analysis was used to measure the relative levels of gene expression. The amplification was performed on ABI Prism 7900-HT Sequence Detection System and Universal MasterMix (Applied Biosystems). The relative levels of the mRNA were calculated with GAPDH mRNA levels as the invariant control (23).

Western blot—Proteins were size-fractionated electrophoretically using sodium dodecyl sulfate-polyacrylamide gel electrophoresis (SDS-PAGE) gels and transferred to polyvinylidene fluoride membranes. The membranes were incubated with the primary and secondary antibody and visualized using an enhanced chemiluminescence detection system (ECL, Cell Signaling Technology Inc). Anti- β -actin (Cell Signaling Technology Inc) was used for equal protein loading.

ABCG1 mRNA Stability—For mRNA stability measurements, actinomycin D

(Act D, 5 mg/ml) was used to inhibit gene transcription. At the indicated time points after the addition of Act D, cells were harvested and total RNA was extracted. The expression levels of ABCG1 at each time point were measured by Northern blot and quantitative RT-PCR and normalized to the GAPDH levels. The remaining mRNA was determined by comparison with the expression level of the relevant gene at the zero time point (designated 100%) when Act D was added (24).

ABCG1 3'-Untranslated Region Constructs. Segments of the human ABCG1 3' untranslated region (UTR) were PCR-amplified using oligonucleotide primers containing flanking *SpeI* recognition sequences and human genomic DNA as a template. The PCR products were gel-purified and ligated downstream of the firefly luciferase coding region of the pGL3-Control vector (Promega). The pGL3-Control vector was chosen because it contains the SV40 promoter without enhancers; changes in luciferase activity can be attributed to the effect of 3'-UTR inserts. The following primers were used to amplify the 3'-UTR of human ABCG1:

forward,
5'-GACTAGTGTACAAAATCCGGGCA
GAGA-3'; reverse,
5'-GACTAGTGCTTAAA
ATAAGAAGCACGTGGA-3'. To create
the mutant ABCG1 3'-UTR
(LUCΔ3'UTR) that containing no
3'-UTR, we cut plasmids with ?? to
remove the ARE-containing region and
religated the remaining vector with the
5' proximal region of UTR. All
constructs were sequenced and the
correct clones were further propagated
to isolate plasmid DNA (25).

Adenoviruses—The adenoviral vector
expressing a dominant-negative AMPK α
mutant (Dn-AMPK) and a constitutively
active form of AMPK (Ca-AMPK) were
kindly donated as a gift by Dr J. Ha
(Department of Molecular Biology,
Kyung Hee University, College of
Medicine, Seoul, Korea) (26).

LXR Reporter Gene Assay—LXR
response element (LXRE)-driven
luciferase reporter vector (LXRE-tk-Luc)
was kindly provided by David J.
Mangelsdorf (27) (UT Southwestern
Medical Center). For LXR activation
studies, 0.75 μ g of LXR response
element (LXRE)-driven luciferase

reporter vector (LXRE-tk-Luc) and 0.75
 μ g of β -galactosidase control vector
(Promega) were used. Six hours after
transfection, cells were treated with
AICAR for 12 h. Luciferase and
 β -galactosidase activities were
determined in cell lysates. The amount
of luciferase activity was normalized for
 β -gal and reported as relative light units
(RLU).

DiI-HDL Binding—The cultured cells
were incubated with different
concentrations of AICAR for 24 h. After
then, the cells were incubated with 5
 μ g/ml DiI-HDL for another 4 h. The
cells were detached using cell removal
buffer containing EDTA, washed and
resuspended the cells in FACS solution
(PBS with 0.5% BSA and 0.02% sodium
azide) at a density of 1×10^6 cells/ml.
The mean fluorescence intensity (MFI)
was analyzed by FACS (FACSort,
Becton Dickinson) (28).

Small Interfering RNA
(*siRNA*)—Complementary RNA (cRNA)
oligonucleotides derived from mouse
ABCG1 sequence (ONTARGET $plus$
SMARTpool targeting mouse ABCG1)
were obtained from Dharmacon
(Chicago, USA) and used to knockdown

ABCG1 expression in macrophages. Scrambled oligonucleotides (ONTARGETplus siCONTROL Non-Targeting Pool) were used as control. Expression levels of ABCG1 in transfected cells were determined by real-time PCR and Western blot.

AMPK kinase activity assay—AMPK kinase activity was measured by using a non-radioisotopic kit from MBL International Corporation according to the provided protocol (Woburn, MA, Cat# CY-1182).

ERK activation—Macrophages lysed with phospho-Tyr protecting lysis buffer (1% Triton X-100, 10% glycerol, 50 mM NaCl, 50 mM HEPES, 2 mM EDTA, 1 mM Na₃VO₄, 10 mM NaF, 10 mM NaPO₄, 10 mM *p*-nitrophenyl phosphate, 10 mM β-glycerol phosphate, and protease inhibitor cocktail). Samples were subjected to SDS-PAGE and immunoblotted with anti-phospho-ERK1/2 and anti-total-ERK1/2 antibodies (Cell Signaling Technology).

Mice and Procedures—Animal experiments were conducted in accordance with institutional guidelines of Sun Yat-sen University. Male apoE

deficient (apoE^{-/-}) mice at 6 wks of age (C57BL/6J genetic background; Jackson Laboratories) were used for this study. The animals were maintained in a 22°C room with a 12 h light/dark cycle and received drinking water ad libitum. The mice were fed on a standard purified mouse diet (AIN-93G) for two weeks prior to the start of experiment. Then, the animals were switched to high-fat diet for 12 wks (HFD, containing 21% fat) receiving either AICAR (*n* = 10, 200 mg · kg⁻¹ · d⁻¹) or vehicle (*n* = 10, 0.9% NaCl) via subcutaneous injection once daily.

Isolation of Mouse Peritoneal Macrophages—To harvest mouse peritoneal macrophages, the mice were sacrificed and ice cold PBS was injected into the peritoneal cavity of each mouse. This fluid was carefully collected and centrifuged at 3000 rpm. Then the supernatant was withdrawn and the cell pellet was resuspended in RPMI 1640 medium and allowed to adhere for 3 h, then washed three times with pre-warmed PBS to remove non-adherent cells. The medium was then replaced with fresh RPMI 1640 medium for further analysis (29).

Plasma Measurements—Total cholesterol, triglycerides and free fatty acids were determined with colorimetric assay systems (Wako chemicals) adapted for microtitre plate assay. Particle size distribution of the lipoproteins was determined by fast-performance liquid chromatography (FPLC), using pooled samples of plasma as previously described (30). In brief, plasma from mice was subjected to FPLC analysis using a Superose 6 column (Pharmacia Biotech) on an HPLC system model 600 (Waters Chromatography). A 100 μ l aliquot of plasma was injected onto the column and separated with a buffer containing 0.15 M NaCl, 0.01 M Na₂HPO₄, 0.1 mM EDTA (pH 7.4), at a flow rate of 0.5 ml/min. Forty 0.5 ml fractions were collected, and tubes 11–40 were analysed for cholesterol. Fractions 14–17 contain VLDL and chylomicra; fractions 18–24 contain LDL and IDL; fractions 25–29 contain HDL; and fractions 30–40 contain non-lipoprotein-associated proteins.

Statistical Analysis—Continuous data were expressed as mean \pm SEM. Comparison between groups was

performed by Student's paired two-tailed t-test. Two-way analysis of variance (ANOVA) was used to examine differences in response to treatments between groups, with post-hoc analysis performed by the method of Student-Newman-Keuls. $P < 0.05$ was considered significant.

RESULTS

AICAR inhibits the formation of macrophage foam cells

To examine the potential effect of AMPK on foam cells formation, the mouse macrophages were loaded with OxLDL (50 μ g/ml) for 24 h to promote cholesteryl-ester accumulation in the absence or presence of AMPK activator AICAR. Combined treatment with AICAR and OxLDL significantly ameliorated intracellular lipid accumulation in macrophages compared with the OxLDL-loaded cells as determined by Oil red O (Fig. 1A and 1B) and Filipin staining (Fig. 1C and 1D). This reduction in intracellular lipid accumulation was also evidenced by direct measurements. AICAR treatment significantly reduced cholesterol accumulation in OxLDL-loaded macrophages (Fig. 1E). These data

suggest that AICAR confers a protective role in the formation of macrophage foam cells.

We also assessed the AMPK activation in this cellular model. Compared with untreated control, AICAR treatment strikingly stimulated the Thr-172 phosphorylation of AMPK, which is an essential marker of AMPK activity (Supplement Fig. 1A). Consistent with this result, AICAR strongly stimulates AMPK enzymatic activity (approximately 2 fold) in macrophages (Supplement Fig. 1B).

AICAR induces expression of ABCG1 in macrophages

ABCG1, ABCA1, SR-A, CD36 and SR-BI have shown their crucial role in cholesterol homeostasis during foam cell formation (6-10,31,32). We therefore delineated the mechanism of AMPK to attenuate lipid accumulation by examining the alterations of these receptors and transporters. Macrophages treated with AICAR (0.5, 1.0 or 2.0 mM) for 24 h showed a dose-dependent induction of ABCG1 mRNA levels as determined by quantitative RT-PCR (Fig. 2A). In accordance with this result,

AICAR treatment also caused a concentration-dependent increase in ABCG1 protein levels (Fig. 2B). However, AICAR did not affect the mRNA (Supplement Fig. 2A-2D) and protein (Supplement Fig. 2E) levels of ABCA1, SR-A, CD36 and SR-BI.

Unrelated AMPK activators, such as metformin (33) and A-769662 (34) were also shown to increase ABCG1 expression in macrophages (Fig. 2C). Furthermore, overexpression of a constitutively active form of AMPK α (CA-AMPK α) led to a robust increase of ABCG1 expression that could not be further enhanced by AICAR. In contrast, when a dominant negative form of AMPK α (DN-AMPK α) was overexpressed, AICAR was unable to enhance ABCG1 expression (Fig. 2D).

We next tested the effects of AICAR on cellular surface binding of HDL to ABCG1, which could account for the higher cholesterol efflux. Dil-HDL binding was increased in a dose-dependent fashion by AICAR incubation (Fig. 2E). Taken together, these data show that AICAR increases the cellular expression of ABCG1 and its interactions with cholesterol

acceptor-HDL.

AICAR did not affect expression of cholesterol synthesis-related genes

We then examined the impact of AICAR on principal target molecules that regulate cellular cholesterol ester synthesis and hydrolysis in macrophages. There was a modest but insignificant reduction in acyl-coenzyme A: cholesterol-acyltransferase 1 (ACAT1), a key enzyme of cholesterol esterification, in the AICAR-treated macrophages (Supplement Fig. 3A) but no effect of AICAR was observed on the expression of hormone-sensitive lipase (HSL) (Supplement Fig. 3B), which acts as the neutral cholesterol esterase, in macrophages.

We also investigated the effect of AICAR on endogenous cholesterol synthesis-related gene expression. Our data showed that AICAR exposure did not alter the mRNA expression of sterol regulatory element binding protein (SREBP) 1 (Supplement Fig. 3C) and SREBP2 (Supplement Fig. 3D), 2 key transcription factors regulating multiple genes involved in the synthesis and metabolism of cholesterol and fatty acids. Additionally, neither

3-hydroxy-3-methylglutaryl coenzyme A reductase [HMGCR] (Supplement Fig. 3E) nor LDL receptor (Supplement Fig. 3F) was influenced by AICAR treatment.

AICAR induces HDL-mediated cholesterol efflux from macrophage foam cells

We next investigated the effects of AICAR on HDL-mediated cholesterol efflux in macrophage foam cells. The OxLDL-loaded macrophages were treated with AICAR for 24 h, and subsequently exposed to HDL. After 24 h, the change of intracellular cholesterol levels was measured. Cholesterol efflux from macrophage foam cells was dose-dependently increased in the presence of AICAR (Fig. 3A). To demonstrate that the variation of intracellular lipids was not due to the action of AICAR on *de novo* cholesterol synthesis, we loaded macrophages with 250 μ Ci [3 H]cholesterol plus OxLDL (50 μ g/ml) for 24 h and determined HDL-mediated efflux of cholesterol by measuring the appearance of cholesterol in the medium. AICAR treatment increased [3 H] cholesterol release in a concentration-dependent fashion

compared to untreated cells (Fig. 3B). Transfection with a dominant-negative AMPK mutant (Fig. 3C) or coincubation with compound C (Fig. 3D), a selective potent inhibitor of AMPK, largely abolished the positive effects of AICAR on cholesterol transport. These data suggest that AMPK confers a protective role in the formation of macrophage foam cells by promotion of cholesterol efflux. Treatment with AICAR did not elicit any release of lactate dehydrogenase (data not shown), ruling out that its effect on cholesterol efflux from foam cells were due to cellular toxicity.

To determine whether enhanced cholesterol efflux following AICAR treatment requires an increase in ABCG1, we transfected the specific ABCG1 siRNA in macrophages to knockdown ABCG1 expression. Western blot analysis revealed that ABCG1 protein expression is effectively suppressed by siRNA, but control siRNA had no such effect (Fig. 3E). ABCG1 silencing significantly reduced cholesterol mass efflux induced by AICAR (Fig. 3F). This result strongly suggests that ABCG1 transporter is

responsible for facilitating cholesterol efflux induced by AMPK activation.

AICAR Regulates ABCG1 mRNA Stability in Macrophages

To further determine the potential mechanism for the induction of ABCG1 expression, we determined the nuclear protein level of LXR α and retinoid X receptor (RXR) in AICAR-treated macrophages. However, AICAR treatment did not affect the nuclear level of LXR α and RXR (Supplement Fig. 4A). Furthermore, AICAR did not influence the LXR α activation by assessing LXRE-mediated luciferase activity (Supplement Fig. 4B). Moreover, coincubation with GGPP, a pharmacological LXR antagonist or LXR small interfering RNA (siRNA) did not affect the induction of ABCG1 by AICAR (Supplement Fig. 4C). These findings imply that LXR α activation did not play the essential role of in AICAR-regulated gene expression of ABCG1 in macrophages.

To further explore the mechanisms by which AICAR increased ABCG1 mRNA levels in macrophages, actinomycin D was added to both vehicle- and AICAR-treated

macrophages for specified periods, and the half-life of ABCG1 mRNA was determined by quantitative RT-PCR in each case. Based on the observed decay values, we found that AICAR prolongs the turnover rate of ABCG1 transcripts by approximately 3-fold (177 min vs 68 min, Fig. 4A).

A central mechanism that controls synthesis of ABCG1 protein involves rapid degradation of the ABCG1 transcript (42). Posttranscriptional regulation of ABCG1 expression has been shown to be mediated through the 3'UTR of ABCG1 mRNA. To determine whether the 3'UTR of ABCG1 regulates its expression in macrophages, we transfected J774.1 macrophages with LUC/3'UTR reporter constructs containing the full-length ABCG1 3'UTR (LUC+3'UTR) or with ABCG1 3'UTR deleted (LUC Δ 3'UTR), and LUC expression was measured. As in Fig. 4B, ABCG1 3'UTR reduced LUC expression approximately 8-fold in macrophages, consistent with rapid decay of the mRNA. We next investigated the ability of AICAR to influence posttranscriptional regulation mediated through ABCG1 3'UTR. Macrophages

transfected with the LUC+3'UTR construct or LUC Δ 3'UTR construct yielded similar levels of expression when the cells were incubated in culture medium. In contrast, addition of AICAR increased LUC expression 7-fold in LUC+3'UTR-transfected macrophages but this response was not observed in LUC Δ 3'UTR-transfected cells (Fig. 4C). These findings indicate that AICAR promote ABCG1 expression through inhibition of rapid mRNA decay mediated by the 3'UTR of the ABCG1 transcript.

ERK Activation is the Prerequisite for AICAR to Increase ABCG1 Expression

To further identify the potential signaling pathway involved in AMPK-mediated upregulation of ABCG1 expression, the different kinase inhibitors, including the inhibitor of MEK1 U0126, the p38 kinase inhibitor SB203580, the c-Jun N-terminal kinase inhibitor curcumin, the PI3 kinase inhibitor wortmannin and the PKC inhibitor calphostin C were used. We found that the induction of ABCG1 mRNA expression by AICAR was most sensitive to the U0126. U0126

incubation almost completely abolished the activity of AICAR on ABCG1 mRNA expression, as confirmed by real-time quantitative PCR (Fig. 5A). The effect of U0126 was also confirmed in CA-AMPK-transfected macrophages (Fig. 5B). However, SB203580, curcumin, wortmannin and calphostin C could not influence the impact of AICAR on macrophage ABCG1 expression (data not shown).

To further determine whether AICAR directly activates the MEK1-ERK pathway, the cultured macrophages were treated with AICAR for different intervals and assessed the levels of activated ERK in control and AICAR-treated cells. AICAR rapidly activated ERK and the kinetics of ERK activation preceded the upregulation of ABCG1 expression by AICAR (Fig. 5C). Exposure to AICAR also dose-dependently activated ERK phosphorylation compared to untreated quiescent macrophages (Fig. 5D). These data indicate that activation of ERK pathway is a prerequisite event in AICAR-mediated stabilization of the ABCG1 transcript.

AICAR Induces ABCG1 Expression

and Attenuates Atherogenesis in ApoE^{-/-} Mice

Finally, we evaluated the impact of chronic AICAR treatment on ABCG1 expression, macrophage foam cell formation and atherosclerotic lesion area. Six-week-old apoE^{-/-} mice fed high fat diet were randomized to receive either AICAR or vehicle for 12 wks. We then isolated mouse peritoneal macrophages and examined the ABCG1 expression. The protein expression of ABCG1 was significantly higher in AICAR-treated macrophages compared with vehicle-treated macrophages (Fig. 6A and 6B). Moreover, OxLDL-induced lipid accumulation was markedly attenuated in AICAR-treated macrophages, and this suppressive effect was abolished by pretreatment with compound C or ABCG1 siRNA (Fig. 6C-6D). Furthermore, we analyzed the development of atherosclerotic lesion in the aortic sinus. Treatment with AICAR markedly diminished the size of atherosclerotic plaques (Oil Red O staining) by $42.60 \pm 9.53\%$ (Fig. 6E and 6F). All the biological parameters were not altered significantly by AICAR treatment in apoE^{-/-} mice (Tab. 1).

Examination of the distribution of cholesterol among the serum lipoprotein fractions revealed similar lipoprotein profiles between the groups (Supplement Fig. 5). These data showed clearly that chronic AMPK activation by AICAR significantly improved the efficiency of macrophage cholesterol transport and ameliorated atherosclerotic lesion formation.

DISCUSSION

Macrophage-derived foam cells are the prominent characteristic in all stages of atherosclerosis (36). These lipid-laden foam cells, present from the earliest discernable fatty-streak lesions to advanced complicated lesion and plaque vulnerability, are key regulators of the pathologic behavior of plaques (37). AMPK is a heterotrimeric enzyme that is expressed in most mammalian tissues. Regulation of fuel supply and energy-generating pathways in response to the metabolic needs of the organism is fundamental functions of this enzyme complex (38,39). Although AMPK signaling pathway is traditionally thought of as an intracellular fuel gauge and regulator of energy metabolism,

recent evidence indicates that it also has vasculoprotective effects such as maintenance of endothelial function (27,40), regulation of the disturbed redox balance (41) and suppression of aberrant endoplasmic reticulum stress (42). However, the effect of AMPK in the transformation of macrophage foam cells, a crucial step for the initiation and progression of atherosclerosis, has never been established. Here, we demonstrated a novel effect of AMPK and its underlying molecular mechanism in suppressing macrophage foam cell formation. We first showed that AMPK activation by AICAR strongly ameliorated the OxLDL-induced foam cell formation. Using this experimental cell culture model, we then uncovered that the beneficial function of AMPK exerted on foam cell formation is dependent on ABCG1. AMPK activator AICAR induces ABCG1 expression in macrophages by regulating ABCG1 mRNA stability via its 3'UTR. At the cellular level, increased ABCG1 expression by AMPK activation promotes cholesterol efflux to HDL from macrophage-derived foam cells, causing a marked reduction of

cholesterol ester accumulation in macrophages. *In vivo* experiments using apoE^{-/-} mice show that AICAR infusion augments ABCG1 expression and reduces the cholesterol content in peritoneal macrophages, thus reducing the area of atherosclerotic plaque. The present study therefore sheds a new light into the potential antiatherogenic properties of AMPK in addition to antioxidative/antiinflammatory functions.

The intracellular lipid homeostasis of macrophage-derived foam cells is dynamically regulated by OxLDL internalization and cholesterol efflux. Macrophage scavenger receptors, particularly the SR-A and CD36, have been implicated in processes that contribute both to early foam cell formation and to the progression toward more complex vulnerable plaques (6,7,43). On the other hand, ABCA1, ABCG1, and SR-BI, the 3 major transporters for cholesterol efflux of foam cells, are pivotal in maintaining the cholesterol homeostasis in macrophages (8-10). Studies using gene-manipulated mice demonstrated that foam cell accumulation and atherosclerotic lesions

are significantly promoted in individual transporter-deficient animals (9,44,45). Therefore, we examined the regulatory role of AICAR on these receptors. Interestingly, AICAR treatment selectively induced both mRNA and protein expression of ABCG1, but not ABCA1, SR-A, CD36, and SR-BI. AICAR treatment was also observed to increase the functional activity of ABCG1 by increasing DiI-labeled HDL binding with macrophages. Furthermore, we found that AICAR treatment did not affect the gene expression of ACAT1, HSL, SREBP1, SREBP2, HMGCR and LDL receptor. Collectively, these data suggest the reduction of macrophage cholesterol accumulation by AICAR is not likely due to the cholesterol uptake and inhibition of endogenous lipid synthesis and hydrolysis, but specifically dependent on ABCG1-mediated cholesterol efflux.

Previous reports suggested that ABCG1 is the LXR-target gene and LXR-mediated transcriptional regulation is required for the induction of this transporter. Beyea (46) and Joseph (47) found that the endogenous LXR ligand 24 (S) 25-epoxycholesterol upregulated

ABCA1 and ABCG1 and that synthetic LXR ligands inhibited the development of atherosclerosis in mice, respectively. However, in this study, neither the LXR α /RXR protein expression nor the LXR α transcriptional activity in macrophages was altered in the presence of AICAR. Furthermore, inhibition of LXR activation by preincubation of macrophages with GGPP or LXR specific siRNA did not reverse the induction of ABCG1 expression by AICAR, indicating that AICAR-mediated upregulation of ABCG1 expression is independent on the activation of LXR α . Thus, the post-transcriptional regulation seems to be the major mechanism underlying the effects of AICAR upon ABCG1 expression. When in the presence of actinomycin D, a general inhibitor of gene transcription, we observed that the mRNA half-life of ABCG1 was considerably extended in AICAR-treated macrophages versus vehicle-treated cells, suggesting that AICAR increased the steady-state expression of ABCG1. We thus sought to understand how AMPK affects the stability of ABCG1 transcripts by examining the ABCG1

mRNA 3'UTR. Based on recent evidence, 3'-UTRs play an important role in mRNA degradation by interacting with microRNA (48). We therefore performed a reporter gene assay using the luciferase constructs containing ABCG1 3'-UTRs to assess a possibility whether AICAR affect these regions. Exposure of macrophages to AICAR markedly restored the attenuated luciferase activity induced by the presence of 3'-UTR, indicating that this region of ABCG1 was actually involved in mRNA stabilization by AICAR. Because ERK activation is required for AICAR-elicited ABCG1 mRNA stabilization, interactions of mRNA binding proteins with these motifs may be a direct downstream event of the ERK signaling cascade and merit further investigation.

Finally, congruous data are observed in the *in vivo* experiment using atherosclerosis-prone apoE^{-/-} mice, which again demonstrated the protective effects of AICAR on foam cells and atherogenesis. The peritoneal macrophages isolated from AICAR-treated apoE^{-/-} mice showed significant increase in ABCG1

expression and reduced lipid accumulation by OxLDL compared with macrophages from vehicle-treated mice. Concominantly, AICAR treatment strongly suppressed the atherosclerotic lesion area. It has recently been shown that AMPK activation suppresses OxLDL-induced proliferation of macrophages (49). It is therefore possible that AICAR inhibits atherosclerosis in part by inhibiting proliferation of lesion macrophages. However we did not observed the evident effects of AICAR on macrophage proliferation in the current study. This is largely due to the OxLDL concentration and incubation time. Ishii N incubated the macrophages with a

lower dose of OxLDL (20 µg/ml) for a long time (6 days), whereas we stimulated macrophages with 50 µg/ml OxLDL for 24 h, which was commonly used to induce cholesterol accumulation in macrophages (18,50,51).

In conclusion, the current study demonstrates a novel mechanistic insight that AMPK exerts anti-atherogenic effects by increasing ABCG1 expression and enhancing HDL-mediated cholesterol efflux from the macrophages. Our findings suggest that AMPK may potentially be of therapeutic value in inhibiting the process of atherosclerotic related cardiovascular disease.

FOOTNOTES

*We greatly appreciate the gift of CA-AMPK and DN-AMPK donated by Dr J. Ha (Kyung Hee University College of Medicine, Seoul, Korea).

This research was supported by grants from the National Natural Science Foundation (No.30730079 and 30700665), grants from the Guangdong Natural Science Foundation (No.9151012003000002), a Foundation for the Author of National Excellent Doctoral Dissertation of PR China (No.200978), Research Fund for the Doctoral Program of Higher Education of China (No.20070558276), the Fundamental Research Funds for the Central Universities of Sun Yat-Sen University (10ykzd04).

The abbreviations used are: AMPK, adenosine monophosphate activated protein

kinase; ABCG1, ATP-binding cassette transporters G1; SR-A, scavenger receptor-A; LXR/RXR, liver X receptor/ retinoid X receptor; ERK, external signal regulated kinase; 3'-UTR, 3' untranslated region; apoE^{-/-} mice, apoE-deficient mice; VLDL, very low density lipoprotein; IDL, intermediate density lipoprotein; LDL, low density lipoprotein; HDL, high density lipoprotein.

REFERENCES

1. Ross, R. (1999) *N. Engl. J. Med.* **340**, 115–126
2. Glass, C.K., and Witztum, J.L. (2001) *Cell.* **104**, 503–516
3. Lusis, A.J. (2000) Atherosclerosis. *Nature.* **407**, 233–241
4. Berliner, J.A., Navab, M., Fogelman, A.M., Frank, J.S., Demer, L.L., Edwards, P.A., Watson, A.D., and Lusis, A.J. (1995) *Circulation.* **91**, 2488–2496
5. Ross, R. (1993) *Nature.* **362**, 801–809
6. Kunjathoor, V.V., Febbraio, M., Podrez, E.A., Moore, K.J., Andersson, L., Koehn, S., Rhee, J.S., Silverstein, R., Hoff, H.F., and Freeman, M.W. (2002) *J. Biol. Chem.* **277**, 49982–49988
7. Rahaman, S.O., Lennon, D.J., Febbraio, M., Podrez, E.A., Hazen, S.L., and Silverstein, R.L. (2006) *Cell. Metab.* **4**, 211–221
8. Wang, N., Silver, D.L., Thiele, C., and Tall, A.R. (2001) *J. Biol. Chem.* **276**, 23742–23747
9. Kennedy, M.A., Barrera, G.C., Nakamura, K., Baldan, A., Tarr, P., Fishbein, M.C., Frank, J., Francone, O.L., and Edwards, P.A. (2005) *Cell. Metab.* **1**, 121–131
10. Tall, A.R., Yvan-Charvet, L., Terasaka, N., Pagler, T., and Wang, N. (2008) *Cell. Metab.* **7**, 365–375
11. Lage, R., Diéguez, C., Vidal-Puig, A., and López, M. (2008) *Trends. Mol. Med.* **4**, 539–549
12. Hardie, D.G. (2007) *Nat. Rev. Mol. Cell. Biol.* **8**, 774–785
13. Hahn-Windgassen, A., Nogueira, V., Chen, C.C., Skeen, J.E., Sonenberg, N., and Hay, N. (2005) *J. Biol. Chem.* **280**, 32081–32089
14. Gleason, C.E., Lu, D., Witters, L.A., Newgard, C.B., and Birnbaum, M.J. (2007)

J. Biol. Chem. **282**, 10341–10351

15. Fisslthaler, B., and Fleming, I. (2009) *Circ. Res.* **105**, 114–127
16. Kahn, B.B., Alquier, T., Carling, D., and Hardie, D.G. (2005) *Cell. Metab.* **1**, 15–25
17. Lowry, O.H., Rosebrough, N.J., Farr, A.L., and Randall, A.J. (1951) *J. Biol. Chem.* **193**, 265–275
18. Lu, K.Y., Ching, L.C., Su, K.H., Yu, Y.B., Kou, Y.R., Hsiao, S.H., Huang, Y.C., Chen, C.Y., Cheng, L.C., Pan, C.C., and Lee, T.S. (2010) *Circulation.* **121**, 1828–1837
19. Rigamonti, E., Helin, L., Lestavel, S., Mutka, A.L., Lepore, M., Fontaine, C., Bouhleb, M.A., Bultel, S., Fruchart, J.C., Ikonen, E., Clavey, V., Staels, B., and Chinetti-Gbaguidi, G. (2005) *Circ. Res.* **97**, 682–689
20. Furuhashi, M., Tuncman, G., Görgün, C.Z., Makowski, L., Atsumi, G., Vaillancourt, E., Kono, K., Babaev, V.R., Fazio, S., Linton, M.F., Sulsky, R., Robl, J.A., Parker, R.A., and Hotamisligil, G.S. (2007) *Nature.* **447**, 959–965
21. Xia, M., Hou, M., Zhu, H., Ma, J., Tang, Z., Wang, Q., Li, Y., Chi, D., Yu, X., Zhao, T., Han, P., Xia, X., and Ling, W. (2005) *J. Biol. Chem.* **280**, 36792–36801
22. Denizot, F., and Lang, R. (1986) *J. Immunol. methods.* **89**, 271–277
23. Pawar, A., Botolin, D., Mangelsdorf, D.J., Jump, D.B. (2003) *J. Biol. Chem.* **278**, 40736–40743
24. Stefulj, J., Panzenboeck, U., Becker, T., Hirschmugl, B., Schweinzer, C., Lang, I., Marsche, G., Sadjak, A., Lang, U., Desoye, G., and Wadsack, C. (2009) *Circ. Res.* **104**, 600–608
25. Dixon, D.A., Tolley, N.D., Bemis-Standoli, K., Martinez, M.L., Weyrich, A.S., Morrow, J.D., Prescott, S.M., and Zimmerman, G.A. (2006) *J. Clin. Invest.* **116**, 2727–2738
26. Sabol, S.L., Brewer, H.B. Jr., and Santamarina-Fojo, S. (2005) *J. Lipid. Res.* **46**, 2151–2167
27. Park, K.G., Min, A.K., Koh, E.H., Kim, H.S., Kim, M.O., Park, H.S., Kim, Y.D., Yoon, T.S., Jang, B.K., Hwang, J.S., Kim, J.B., Choi, H.S., Park, J.Y., Lee, I.K.,

- and Lee, K.U. (2008) *Hepatology*. **48**, 1477–1486
28. Li, D., Zhang, Y., Ma, J., Ling, W., and Xia, M. (2010) *Arterioscler. Thromb. Vasc. Biol.* **30**, 1354–1362
 29. Gu, X., Trigatti, B., Xu, S., Acton, S., Babitt, J., and Krieger, M. (1998) *J. Biol. Chem.* **273**, 26338–26348
 30. Otnad, E., Parthasarathy, S., Sambrano, G.R., Ramprasad, M.P., Quehenberger, O., Kondratenko, N., Green, S., and Steinberg, D. (1995) *Proc. Natl. Acad. Sci. USA.* **92**, 1391–1395
 31. Babaev, V. R., Patel, M. B., Semenkovich, C. F., Fazio, S., and Linton, M. F. (2000) *J. Biol. Chem.* **275**, 26293–26299
 32. Mauldin, J.P., Srinivasan, S., Mulya, A., Gebre, A., Parks, J.S., Daugherty, A., and Hedrick, C.C. (2006) *J. Biol. Chem.* **281**, 21216–21224
 33. Argmann, C.A., Edwards, J.Y., Sawyez, C.G., O'Neil, C.H., Hegele, R.A., Pickering, J.G., and Huff, M.W. (2005) *J. Biol. Chem.* **280**, 22212–22221
 34. Zhou, G., Myers, R., Li, Y., Chen, Y., Shen, X., Fenyk-Melody, J., Wu, M., Ventre, J., Doebber, T., Fujii, N., Musi, N., Hirshman, M.F., Goodyear, L.J., and Moller, D.E. (2001) *J. Clin. Invest.* **108**, 1167–1174
 35. Cool, B., Zinker, B., Chiou, W., Kifle, L., Cao, N., Perham, M., Dickinson, R., Adler, A., Gagne, G., Iyengar, R., Zhao, G., Marsh, K., Kym, P., Jung, P., Camp, H.S., and Frevert, E. (2006) *Cell. Metab.* **3**, 403–416
 36. Shyu, A.B., Wilkinson, M.F., and van, Hoof. A. (2008) *EMBO J.* **27**, 471–481
 37. Li, A.C., and Glass, C.K. (2002) *Nat. Med.* **8**, 1235–1242
 38. Osterud, B., and Bjorklid, E. (2003) *Physiol. Rev.* **83**, 1069–1112
 39. Lim, C.T., Kola, B., and Korbonits, M. (2010) *J. Mol. Endocrinol.* **44**, 87–97
 40. Zhang, B.B., Zhou, G., and Li, C. (2009) *Cell. Metab.* **9**, 407–416
 41. Schulz, E., Anter, E., Zou, M.H., and Keaney, JF. Jr. (2005) *Circulation.* **111**, 3473–3480
 42. Schulz, E., Dopheide, J., Schuhmacher, S., Thomas, S.R., Chen, K., Daiber, A., Wenzel, P., Münzel, T., and Keaney, JF. Jr. (2008) *Circulation.* **118**, 1347–1357
 43. Dong, Y., Zhang, M., Liang, B., Xie, Z., Zhao, Z., Asfa, S., Choi, H.C., and Zou,

- M.H. (2010) *Circulation*. **21**, 792–803
44. Moore, K.J., and Freeman, M.W. (2006) *Arterioscler Thromb Vasc Biol*. **26**, 1702–1711
45. McNeish, J., Aiello, R.J., Guyot, D., Turi, T., Gabel, C., Aldinger, C., Hoppe, K.L., Roach, M.L., Royer, L.J., de, Wet. J., Broccardo, C., Chimini, G., and Francone, O.L. (2000) *Proc. Natl. Acad. Sci. U S A*. **97**, 4245–4250
46. Trigatti, B., Rayburn, H., Vinals, M., Braun, A., Miettinen, H., Penman, M., Hertz, M., Schrenzel, M., Amigo, L., Rigotti, A., and Krieger, M. (1999) *Proc. Natl. Acad. Sci. U S A*. **96**, 9322–9327
47. Beyea, M.M., Heslop, C.L., Sawyez, C.G., Edwards, J.Y., Markle, J.G., Hegele, R.A., and Huff, M.W. (2007) *J. Biol. Chem*. **282**, 5207–5216
48. Joseph, S.B., McKilligin, E., Pei, L., Watson, M.A., Collins, A.R., Laffitte, B.A., Chen, M., Noh, G., Goodman, J., Hagger, G.N., Tran, J., Tippin, T.K., Wang, X., Lusis, A.J., Hsueh, W.A., Law, R.E., Collins, J.L., Willson, T.M., and Tontonoz, P. (2002) *Proc. Natl. Acad. Sci. U S A*. **99**, 7604–7609
49. Ishii, N., Matsumura, T., Kinoshita, H., Motoshima, H., Kojima, K., Tsutsumi, A., Kawasaki, S., Yano, M., Senokuchi, T., Asano, T., Nishikawa, T., and Araki, E. (2009) *J. Biol. Chem*. **284**, 34561–34569
50. Chinetti, G., Lestavel, S., Bocher, V., Remaley, A. T., Neve, B., Torra, I. P., Teissier, E., Minnich, A., Jaye, M., Duverger, N., Brewer, H. B., Fruchart, J. C., Clavey, V., and Staels, B. (2001) *Nat. Med*. **7**, 53–58
51. Conway, J.P., and Kinter, M. (2006) *J. Biol. Chem*. **281**, 27991–28001

FIGURE LEGENDS

FIGURE 1. AICAR attenuates OxLDL-induced lipidaccumulation in macrophages. J774.A1 mouse macrophages were incubated with vehicle (PBS), OxLDL (50 µg/ml) alone, AICAR (1 mM) alone, or a combination of AICAR and OxLDL for 24 h. After fixation by 4% paraformaldehyde, cells were stained with (A and B) Oil Red O or (C and D) filipin, respectively to detect the lipid accumulation, and hematoxylin was used as counterstaining. Magnification × 200. The intracellular lipid level (B and D) was measured by alcohol extraction after staining. (E) The intracellular levels of cholesterol were analyzed by colorimetric assay kits. ** $P < 0.01$.

FIGURE 2. Effects of AICAR on the expression of ABCG1. J774.A1 macrophages were incubated with AICAR (0.5, 1.0, 2.0 mM) for 24 h. (A) Cell lysates were subjected to real-time quantitative PCR to determine ABCG1 mRNA expression. The results are expressed as fold of control from at least three independent assays. (B) Western blot was used to measure the protein levels of ABCG1. The representative blots from three independent experiments are shown. (C) Macrophages were treated with A769662 (100 µM) or metformin (met, 1 mM) for 24 h. (D) Macrophages were infected with adenoviruses encoding constitutively active (CA) or dominant negative (DN) forms of AMPK α in presence of AICAR (1 mM) or vehicle. ABCG1 protein expression was measured by Western blot. The representative blots from three independent experiments are shown. (E) J774.A1 macrophages were incubated with AICAR (0.5, 1.0, 2.0 mM) for 24 h. After then, the cells were incubated with 5 µg/mL DiI-HDL for 4 h, resuspended in FACS solution and analyzed with the FACS flow cytometer. The mean fluorescence intensity (MFI) of untreated cells (control) is expressed as 100%. The data shown are expressed as a percentage of the control from three independent measurements. * $P < 0.05$, or ** $P < 0.01$ compared with control.

FIGURE 3. AICAR enhance HDL-mediated cholesterol efflux in macrophages. (A) Macrophages were loaded with OxLDL (50 µg/ml) alone or in the presence of

different concentrations of AICAR for 24 h. These cells were then washed with PBS and incubated with HDL (20 $\mu\text{g/ml}$) as an acceptor for a further 16 h. Determination of cholesterol efflux from the cells was performed as described in Methods. The results are represented as the mean \pm SEM of three individual experiments. (B) [^3H]cholesterol-loaded macrophages were treated with Cy-3-g or Pn-3-g and subsequently incubated with RPMI 1640 medium with or without AICAR (0.5~2.0 mM) as indicated. HDL-induced [^3H]cholesterol efflux was measured as described. Values are expressed relative to the control, set as 1. Results are the mean \pm SEM of triplicate determinations, representative of 3 independent experiments. * P <0.05 or ** P <0.01 compared with control. (C-D) Cholesterol-loaded macrophages were transfected with (C) DN-AMPK α or pretreated with the (D) compound C (10 mM). The cells were then incubated with AICAR (1 mM) for a further 24 h. HDL-mediated cholesterol efflux was determined as Methods. Results are represented as mean \pm SEM of three individual experiments. ** P <0.01. (E-F) Macrophages were transfected with ABCG1 siRNA or a non-specific control siRNA. (E) Western blot analyses using antibody against ABCG1 and β -actin were performed to test transfection efficiency. Representative blots from 3 independent assays are presented. (F) Twenty-four hours after transfection, the cells were further incubated with OxLDL (50 $\mu\text{g/ml}$) alone or in the presence of AICAR (1 mM) for 24 h. Macrophages were then washed with PBS and incubated with or without HDL (20 $\mu\text{g/ml}$) for 16 h. Results are represented as mean \pm SEM of three individual experiments. ** P <0.01.

FIGURE 4. AICAR regulates ABCG1 mRNA decay through 3'-UTR. (A) Macrophages were left untreated or incubated with AICAR (1 mM) for 24 h and actinomycin D (5 $\mu\text{g/ml}$) was added to the cells for different intervals. Total RNA was then isolated and ABCG1 mRNA was assayed by quantitative RT-PCR and the normalized ABCG1 mRNA signals were plotted as the percentage of the ABCG1 mRNA remaining. Decay curves were plotted versus time. (B) LUC/3'UTR-reporter constructs containing no 3'UTR (LUC Δ 3'UTR) or ABCG1 3'UTR (LUC+3'UTR) were transfected into J774.1 macrophages. LUC activity (RLU) was normalized to

total protein from the three independent experiments. $**P<0.01$ compared with LUCΔ3'UTR. (C) Macrophages were transfected with LUC/3'UTR or LUCΔ3'UTR reporter constructs, respective and kept in culture medium or incubated with 1 mM AICAR. Relative LUC activity was normalized to total protein, and values shown are based on LUC expression from control transfections. $**P<0.01$.

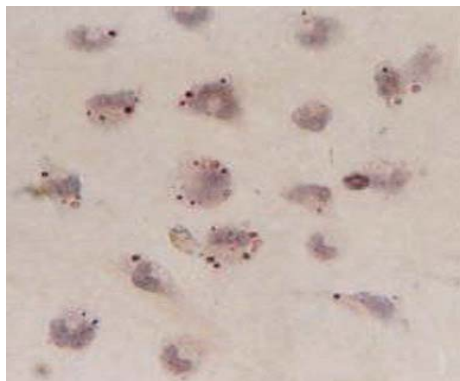
FIGURE 5. Blocking ERK activation abolished the regulatory effect of AICAR on ABCG1. (A) Relative amount of ABCG1 mRNA was measured by a quantitative real-time PCR after macrophages were treated with 1.0 mM AICAR for 8 h in the presence or absence of 0.5 μM U0126. (B) Macrophages were infected with adenoviruses encoding CA-AMPK for 12 h. After then, the cells were incubated with medium or treated with 0.5 μM U0126 for 8 h. The amount of ABCG1 transcript were expressed as fold in untreated control cells (defined as 1), and amounts of ABCG1 mRNA were plotted relative to that value. $*P<0.05$. (C) The cellular lysates were harvested from macrophages that were untreated or treated with AICAR at a dose of 1.0 mM for different intervals as indicated. Total cellular proteins (40 μg/lane) were subjected to SDS-PAGE and Western blot using antibodies specific for either the activated and phosphorylated forms of ERK1/2, or total ERK 1/2. The representative blot from the three independent experiments was shown. (D) J774 macrophages were treated with AICAR for 1 h at the indicated concentrations and total cell lysates were used to detect phosphorylated and nonphosphorylated ERK by Western blot. The representative blot from the three independent experiments was shown.

FIGURE 6. AICAR increases ABCG1 expression and inhibits atherogenesis in apoE^{-/-} mice. ApoE^{-/-} mice, fed a high fat cholesterol diet, were randomly administered with either AICAR ($n = 8$, 200 mg · kg⁻¹ · d⁻¹) or vehicle ($n = 8$, 0.9% NaCl) for 12 wks. (A) The peritoneal macrophages were isolated, lysed and subjected to Western blot to evaluate the protein levels of ABCG1 and β-actin. (B) Quantification of ABCG1 protein relative levels. $**P<0.01$. (C and D) The peritoneal macrophages from vehicle- and AICAR-treated mice were preincubated with compound C or transfected with

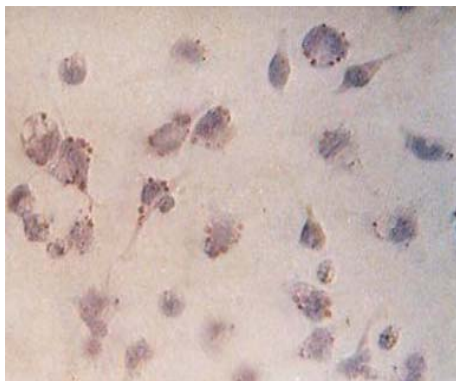
ABCG1 siRNA for 6 h, followed by the treatment of OxLDL (50 $\mu\text{g/ml}$) for an additional 24 h. After incubation, cells were fixed and stained with Oil Red O to detect lipid accumulation. Hematoxylin was used as counterstaining. $**P<0.01$. (E) Determination of atherosclerotic lesion size in apoE^{-/-} mice. The aortic roots of the animals treated as described were analyzed for atherosclerotic lesion size with Oil Red O staining. Magnification $\times 400$. (F) Quantitative analysis of the atherosclerotic lesion areas in the aortic sinus ($n = 8$, $**P<0.01$).

Fig. 1

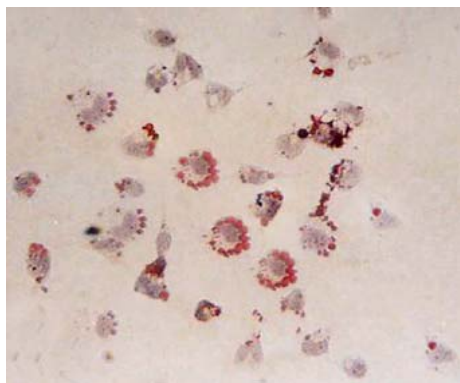
A



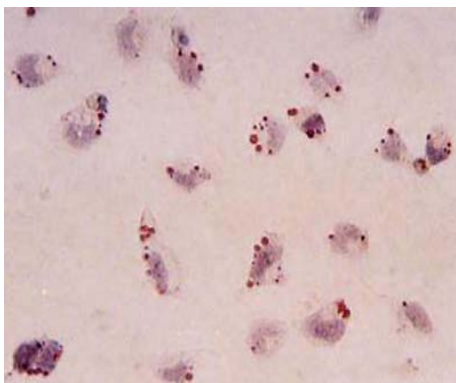
Control



AICAR

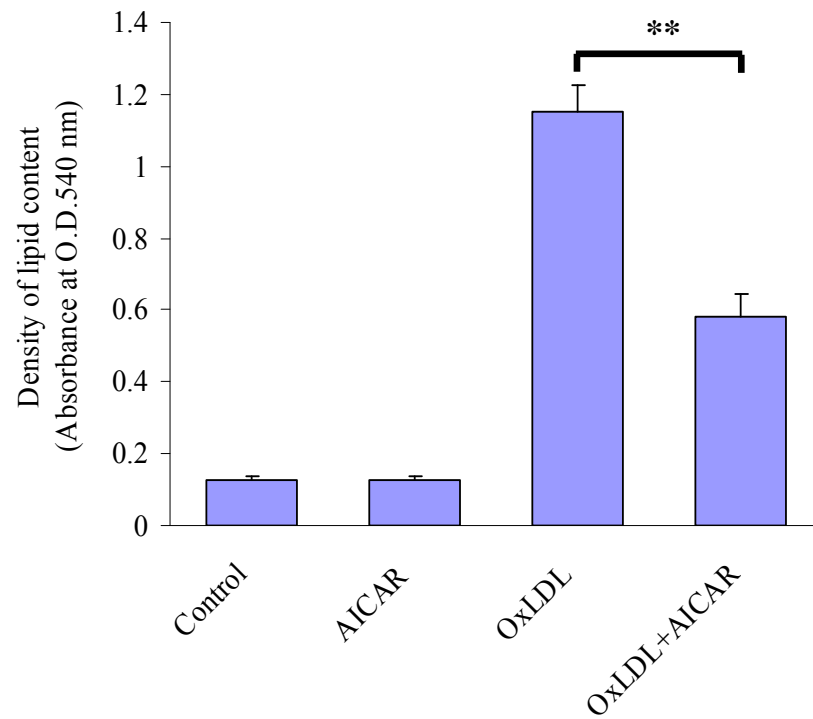


OxLDL

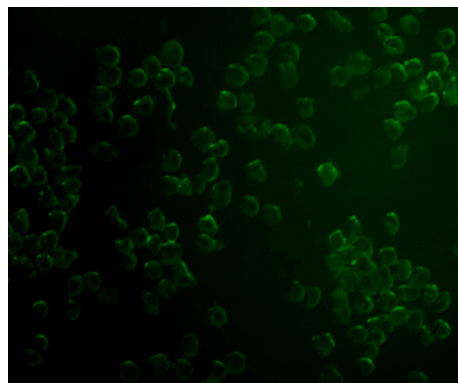


OxLDL + AICAR

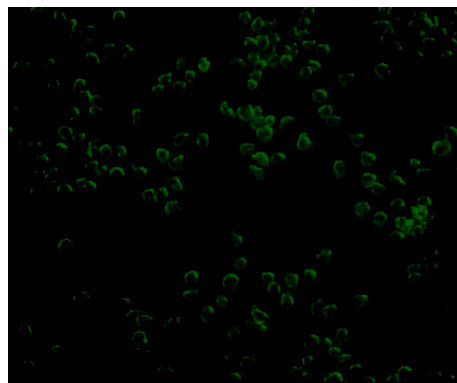
B



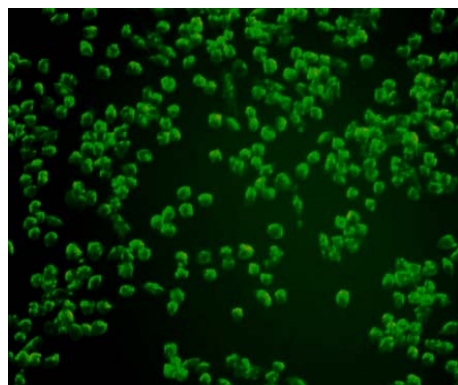
C



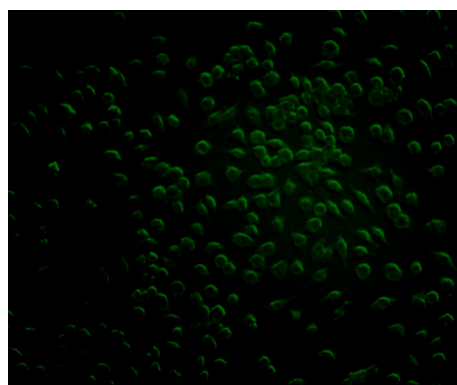
Control



AICAR

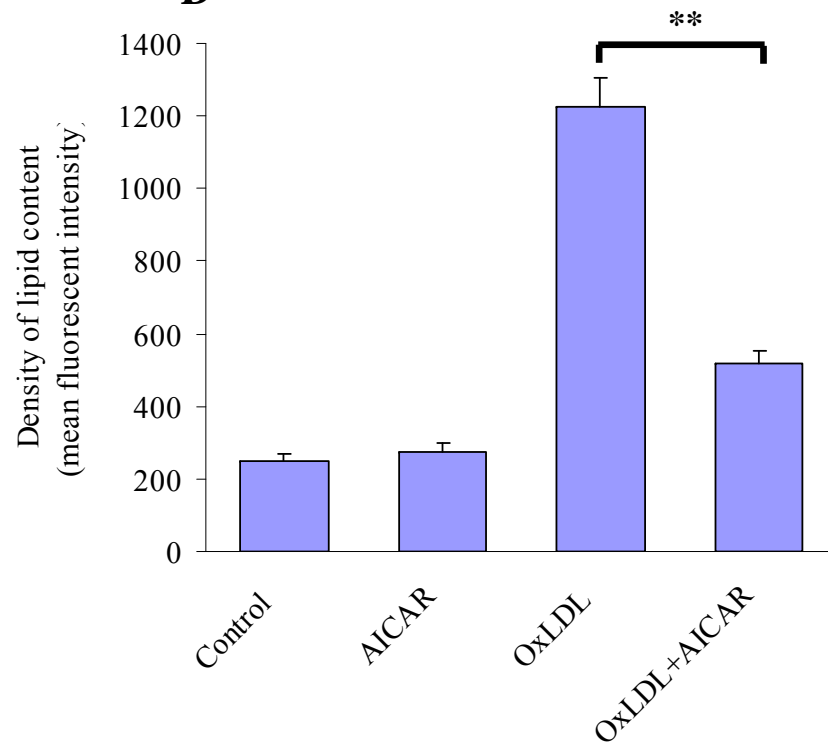


OxLDL



OxLDL +AICAR

D



E

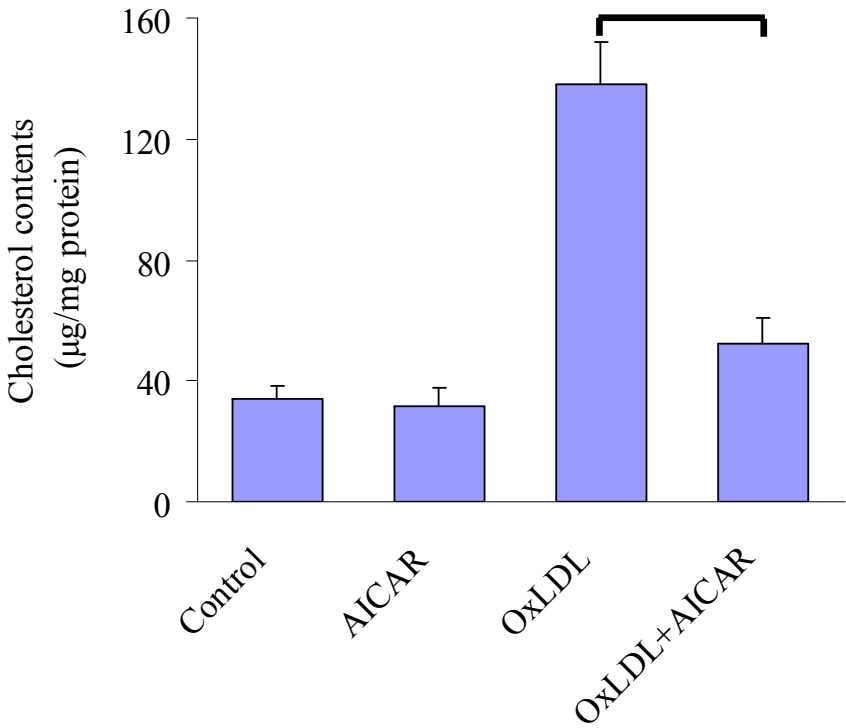
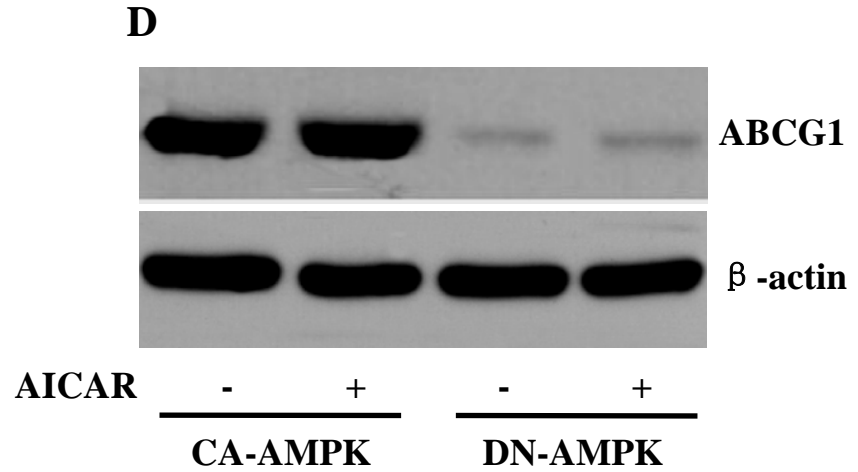
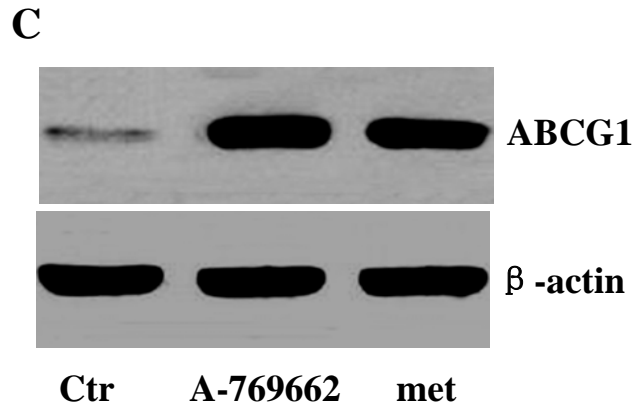
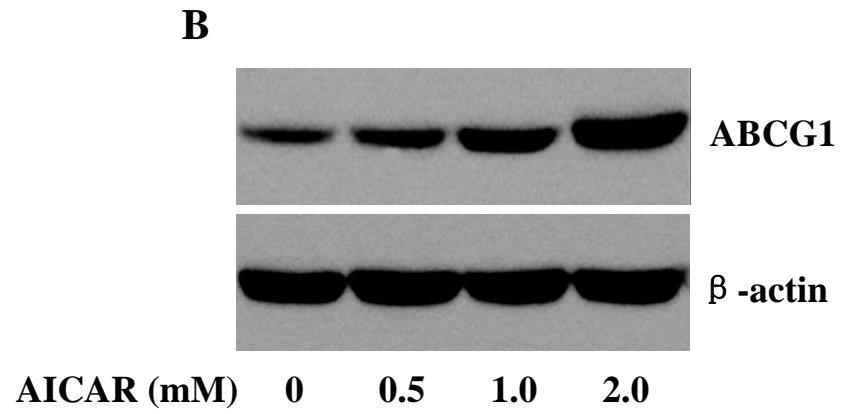
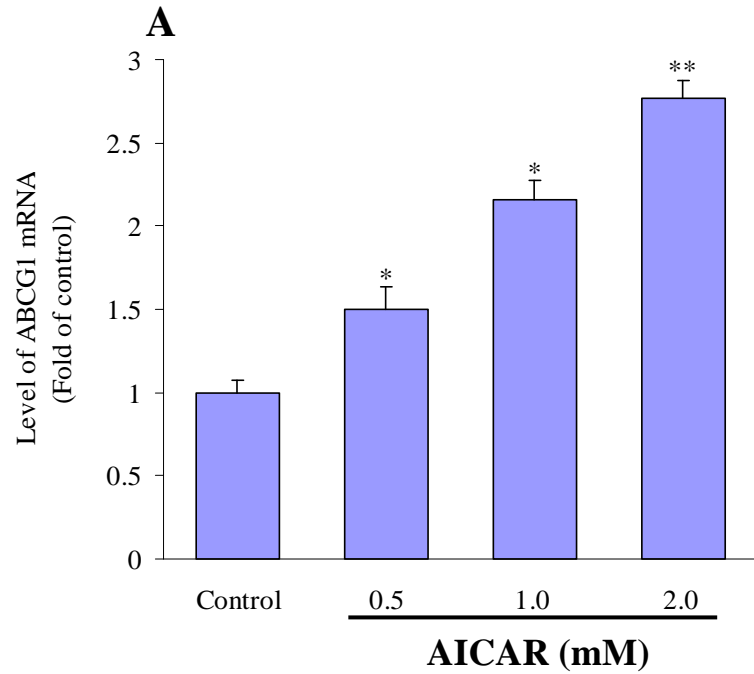


Fig. 2

E

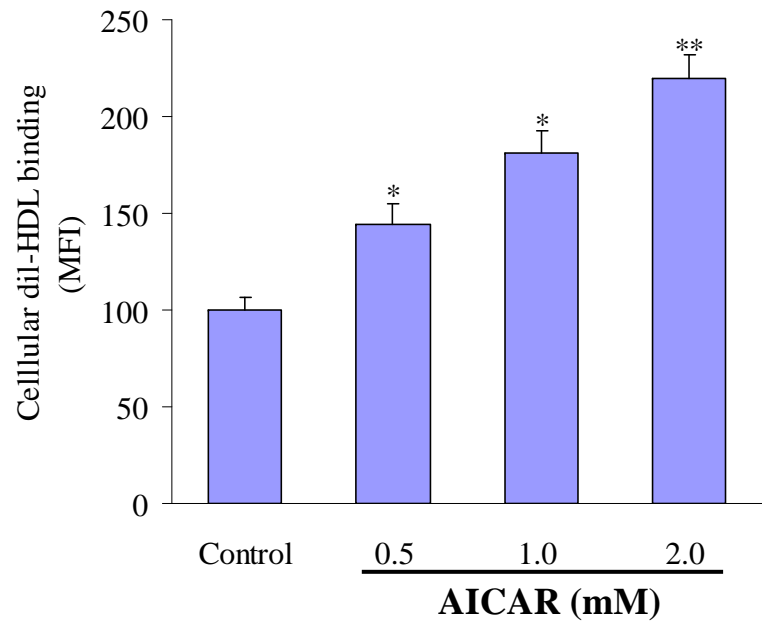
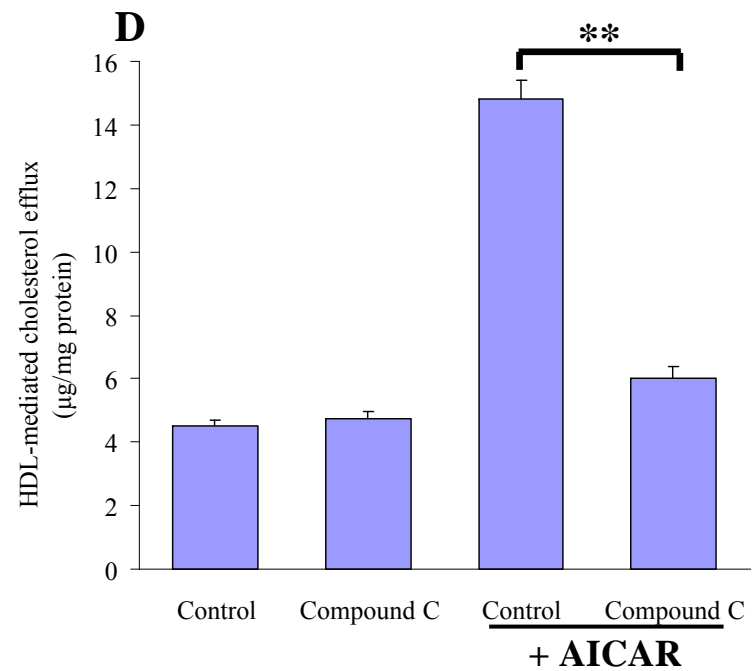
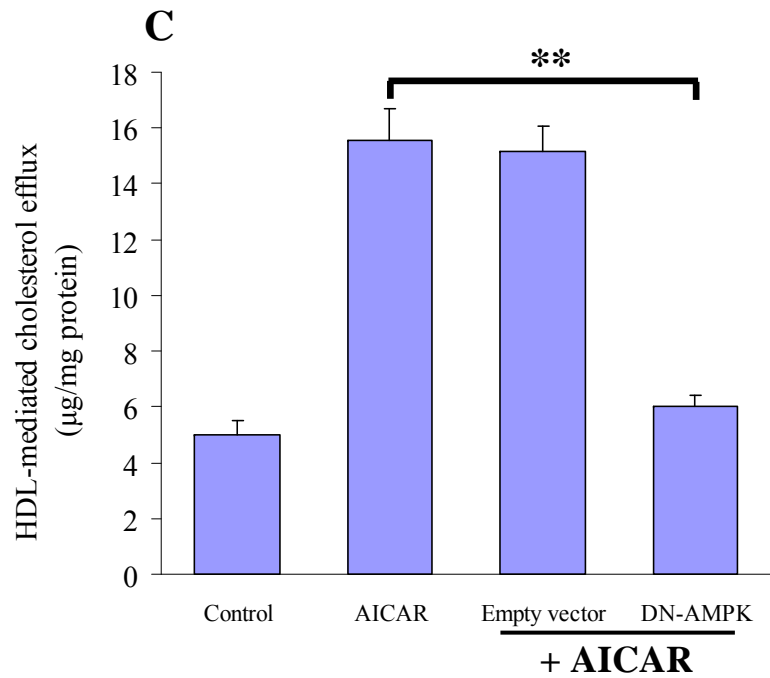
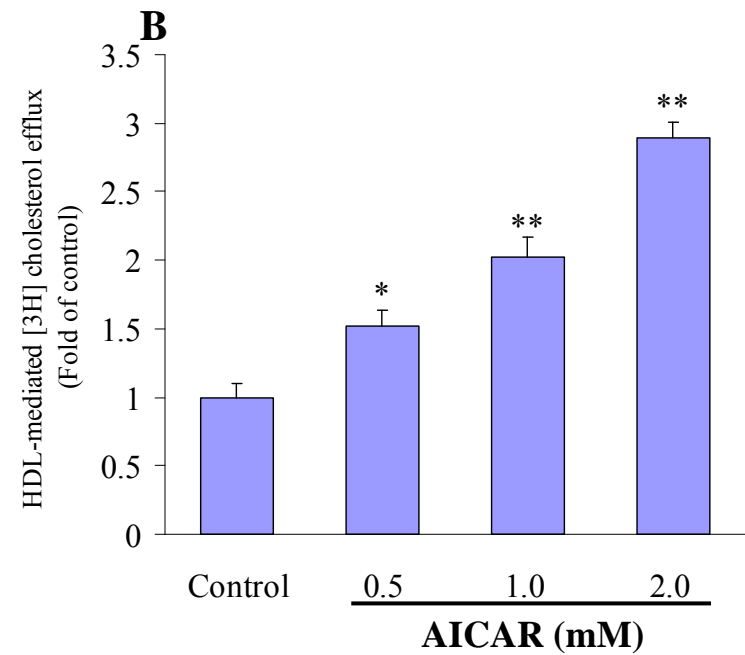
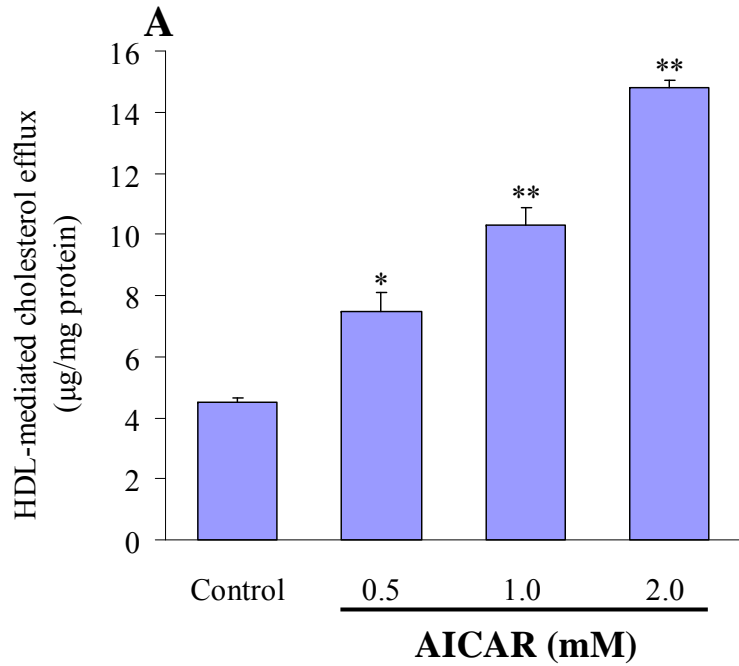


Fig. 3

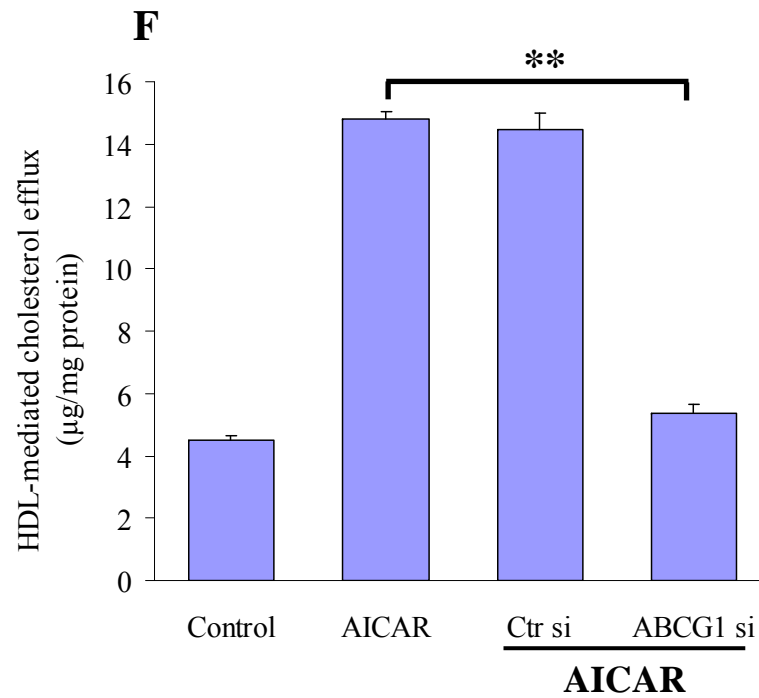
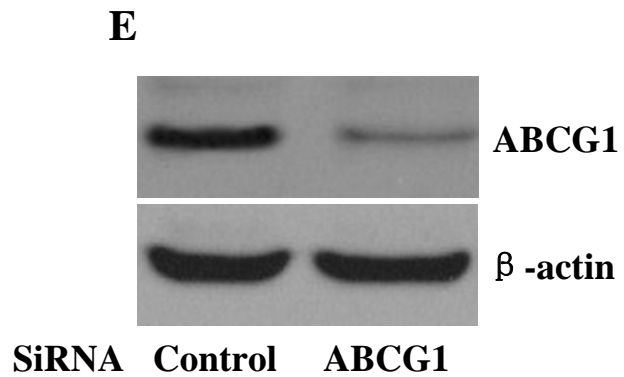


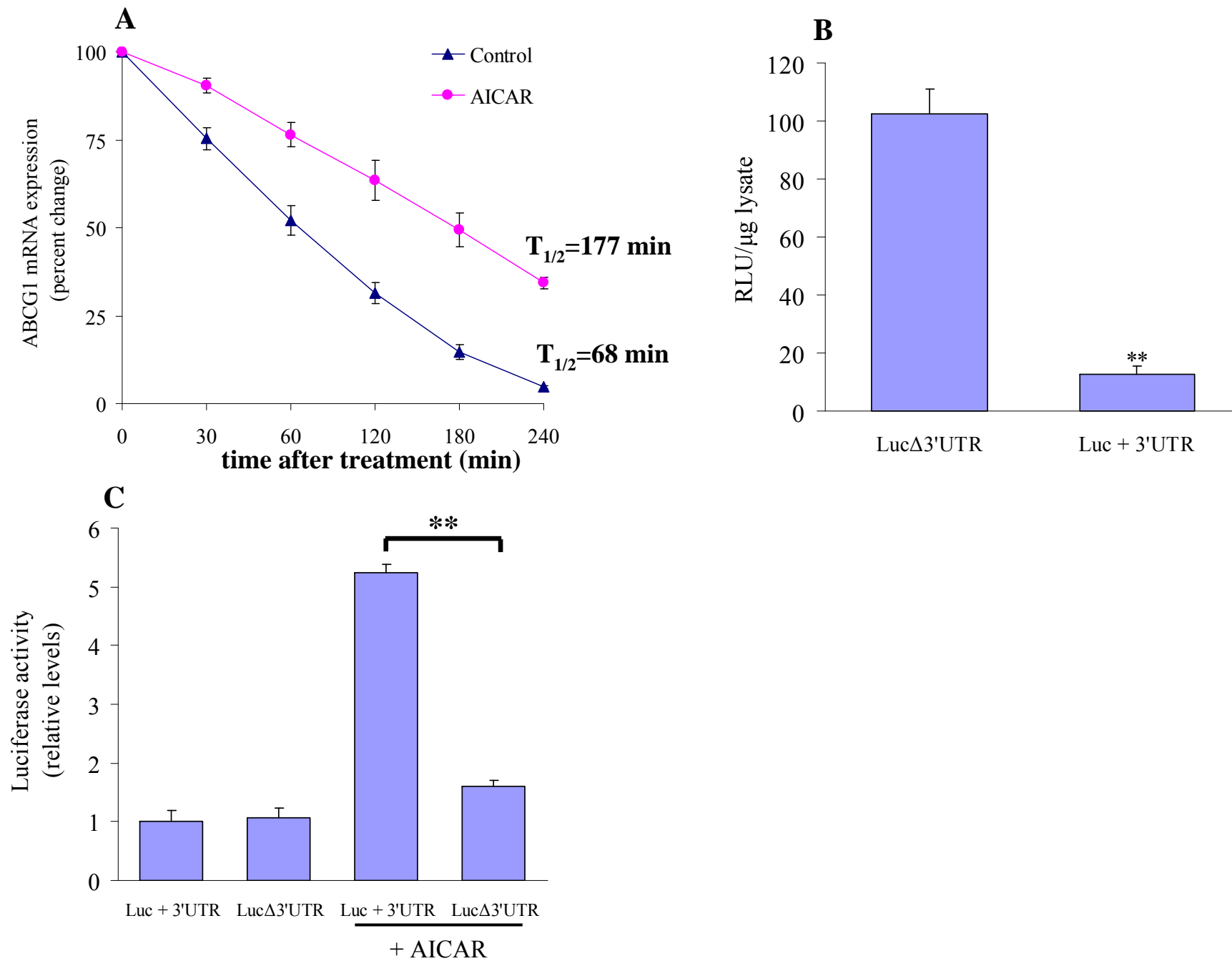
Fig. 4

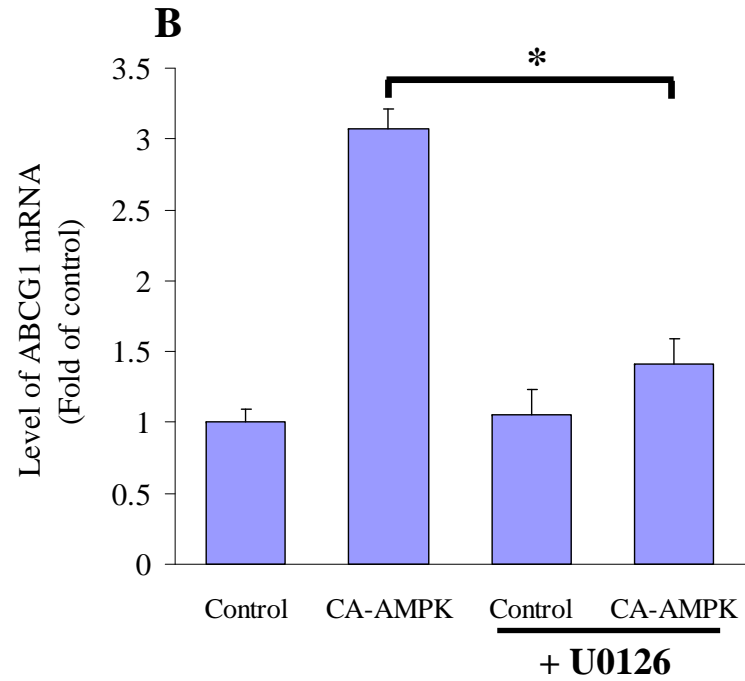
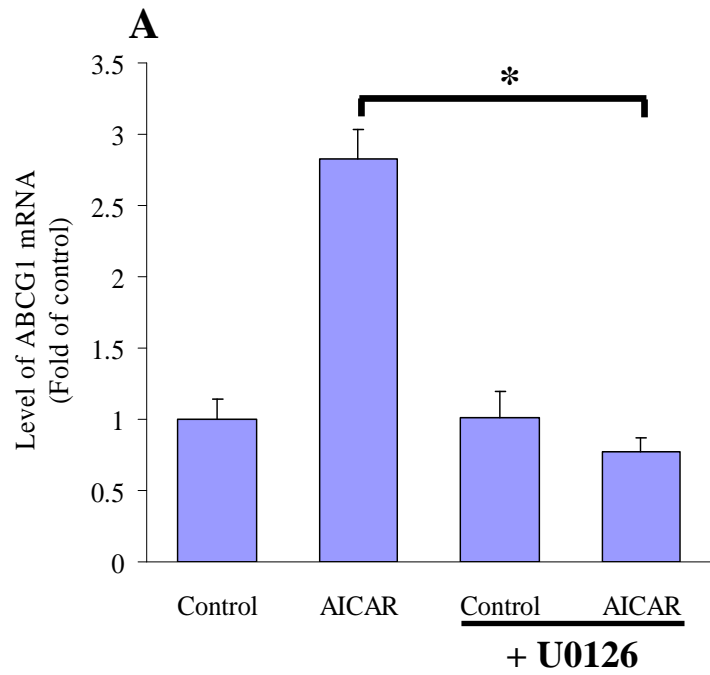
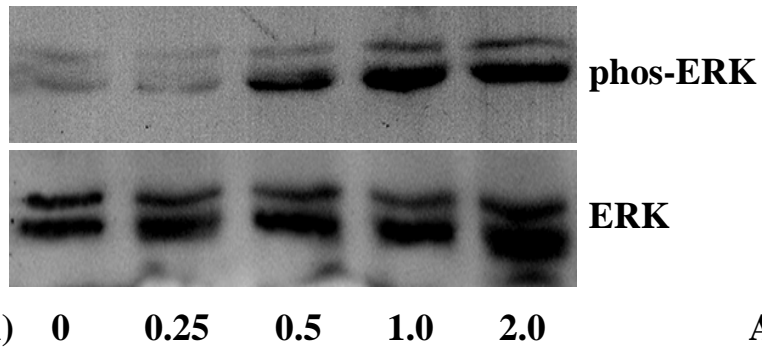
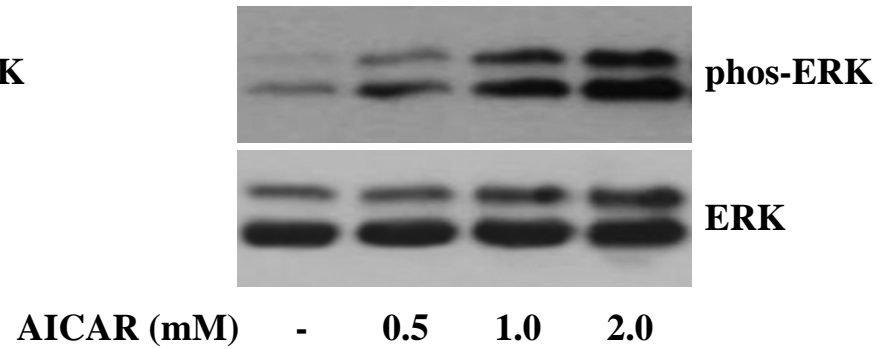
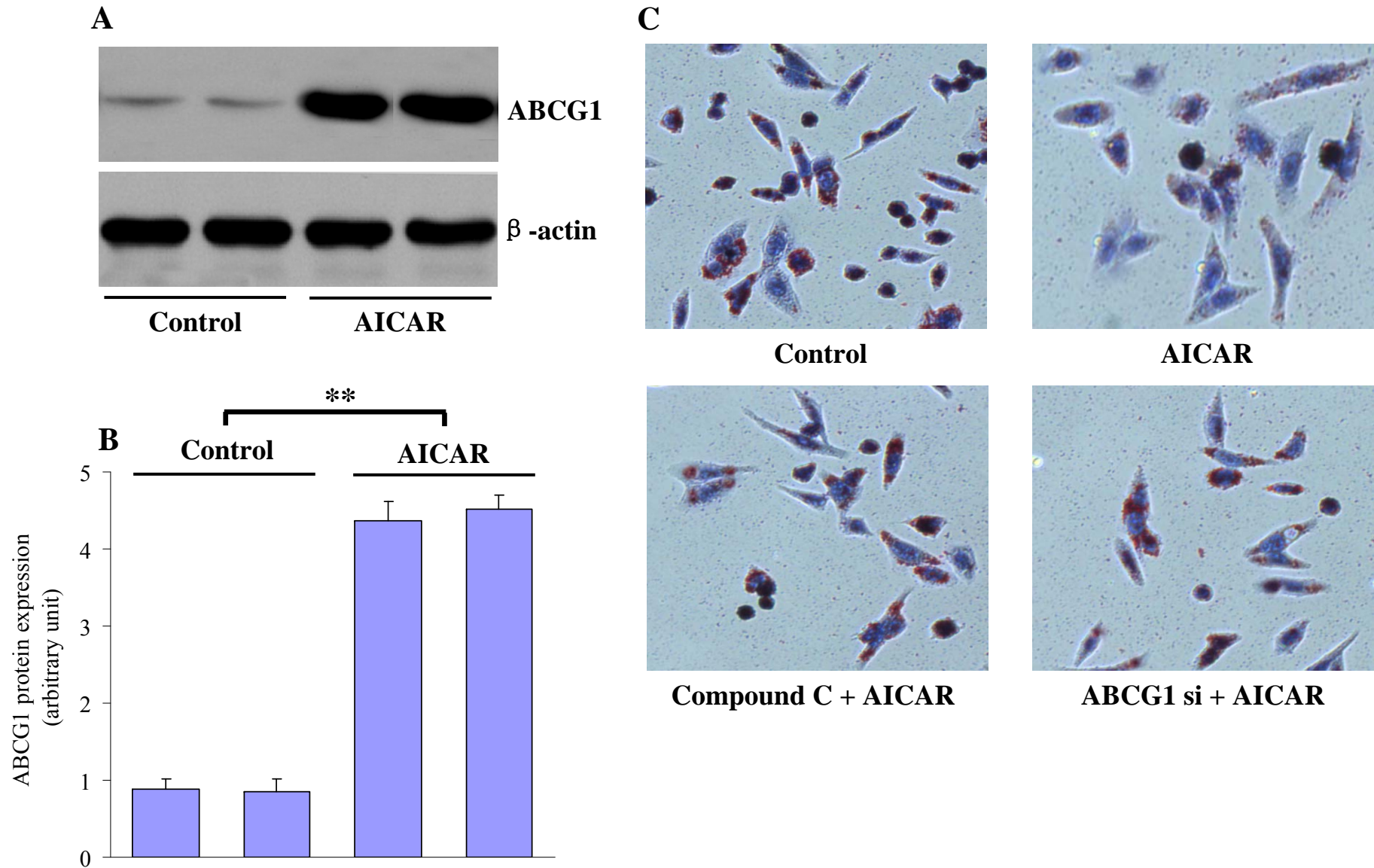
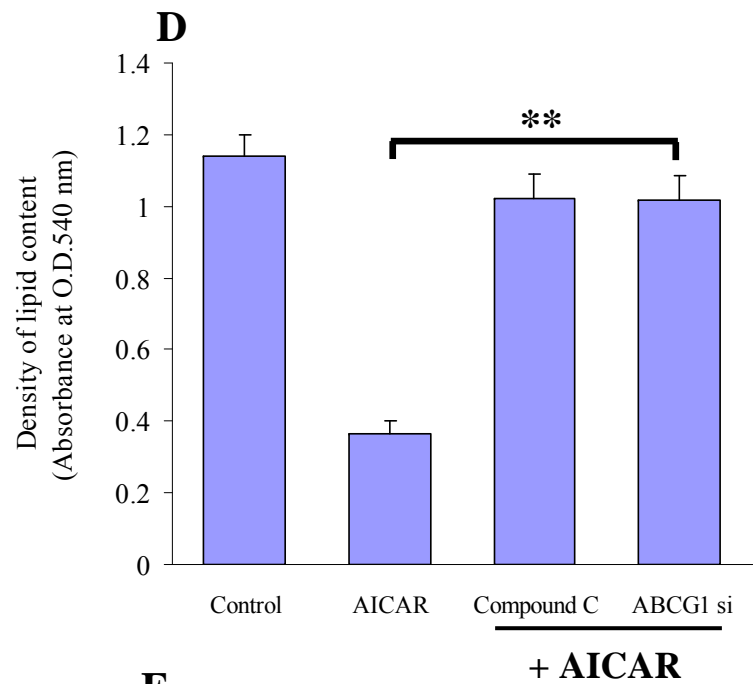
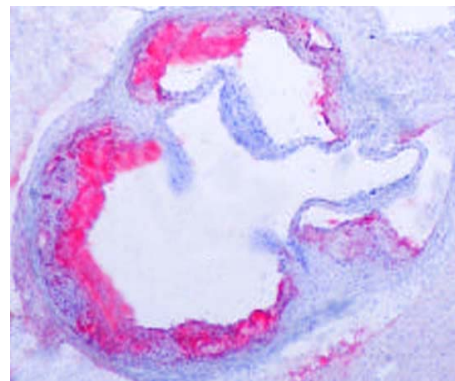
Fig. 5**C****D**

Fig. 6

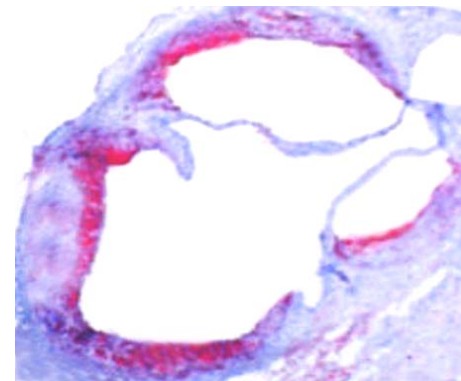




E



Control



AICAR

